

ME 608: Homework 1

Tanmay C. Shidhore

September 19, 2017

1 Problem 1

The following figures (1 through 4) show the screenshots for 4 different meshes A, B, C, D created using ANSYS ICEM CFD. A is the coarsest mesh and the node density is progressively refined in the order B-C-D, with D being the finest grid. The number of elements in these meshes are 302,1020, 4637 and 9020 respectively

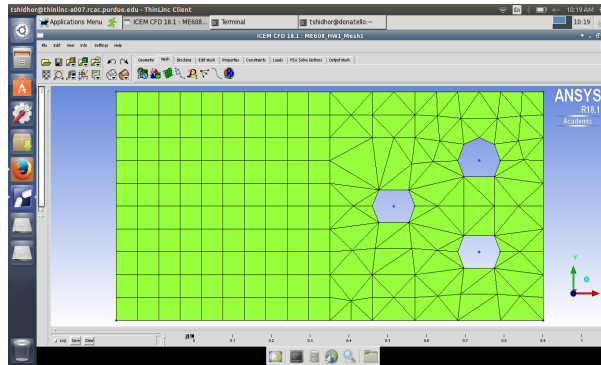


Figure 1: Mesh A

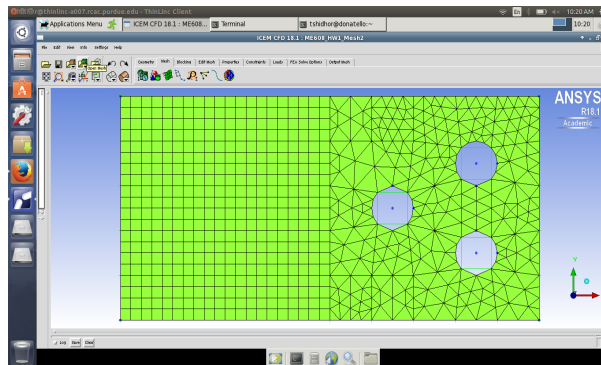


Figure 2: Mesh B

For these meshes, figures 5 through 8 give the corresponding mesh quality, as computed by ICEM CFD. The quad elements in the figures above have the best possible value of mesh quality. As one refines the mesh, a larger number of triangular elements show improved quality. This is apparent from an increase in number of elements marked blue (which represents good quality elements) from Mesh A to Mesh D.

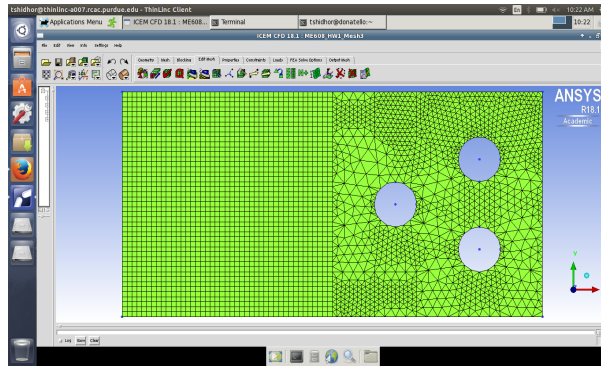


Figure 3: Mesh C

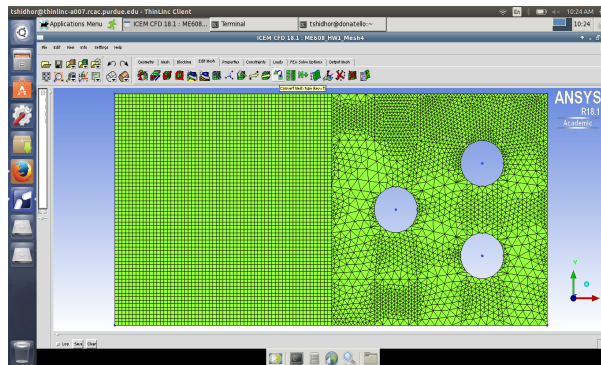


Figure 4: Mesh D

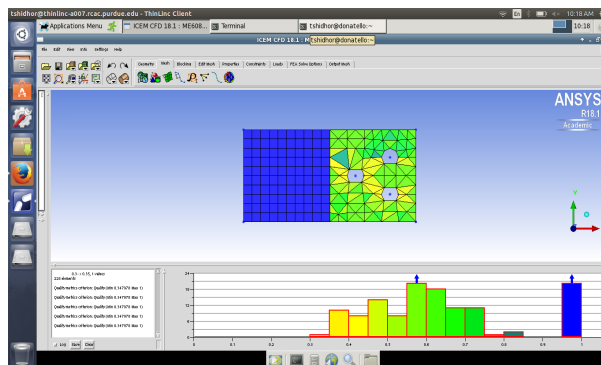


Figure 5: Quality for Mesh A

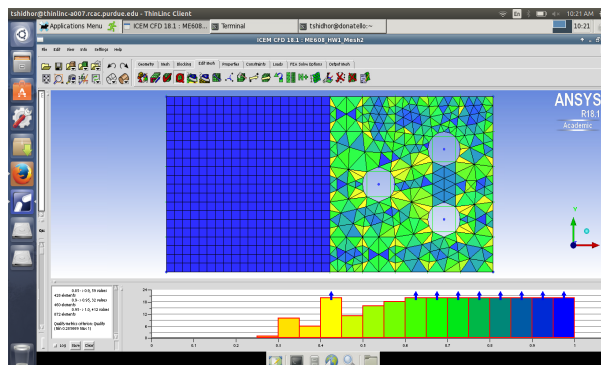


Figure 6: Quality for Mesh B

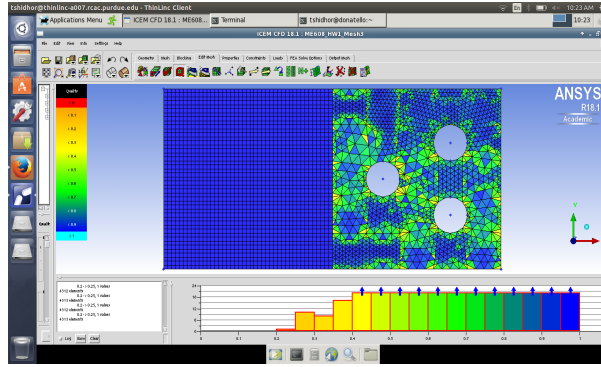


Figure 7: Quality for Mesh C

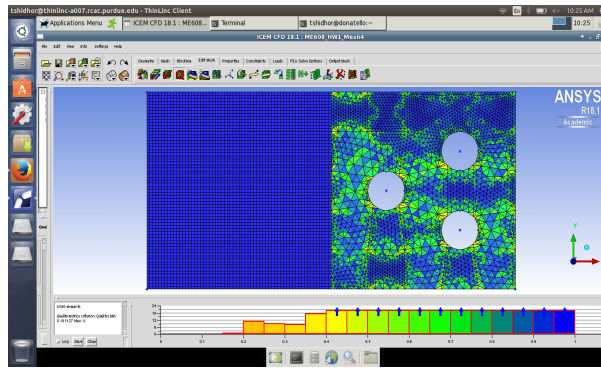


Figure 8: Quality for Mesh D

2 Problem 2

2.1 Part a: Poor Man's heat transfer problem

Mesh C, which is a considerably dense mesh, was considered for this problem. The 3 holes in the right part of the mesh were maintained at 500K. The rectangular boundary and the entire solid was set to 300K. A poor man's heat transfer problem was solved on the above mesh with a convergence criterion of 0.01 for the RMS difference between two successive iterations. The following plots show the evolution of solution in pseudo time at an interval of 500 iterations. The RMS error converges to the specified criteria after 2410 iterations. It should be noted that the values within the three holes themselves have no physical meaning.

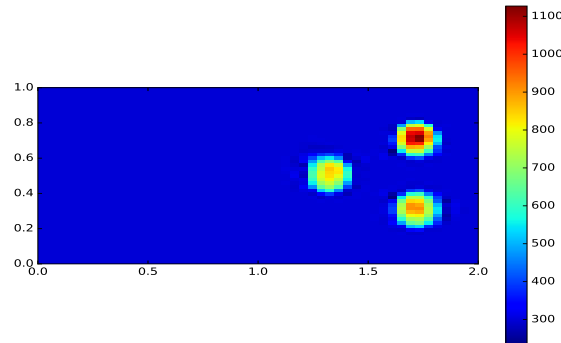


Figure 9: Initial Temperature Field

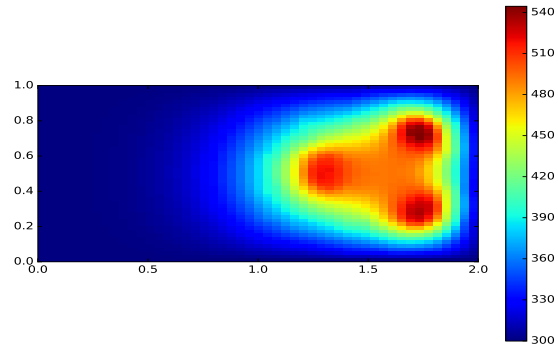


Figure 10: Temperature distribution at 500 iterations

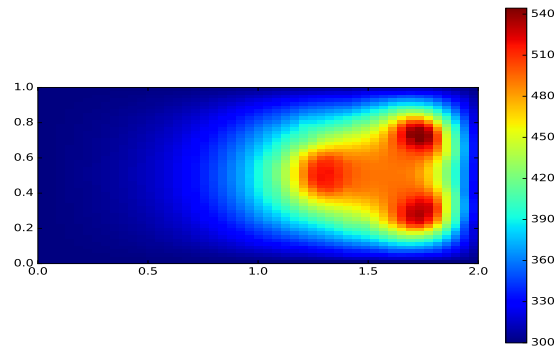


Figure 11: Temperature distribution at 1000 iterations

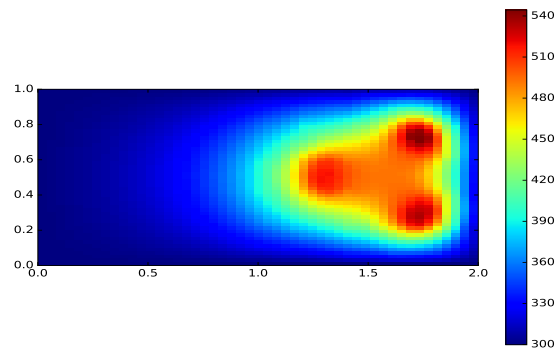


Figure 12: Temperature distribution at 1500 iterations

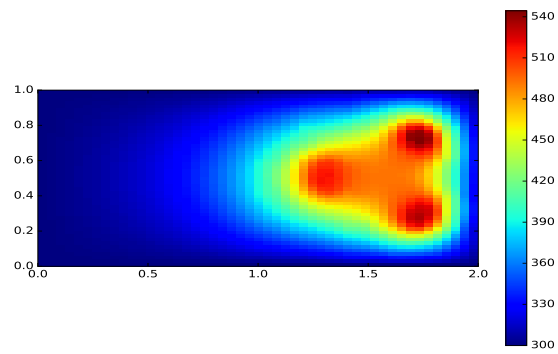


Figure 13: Temperature distribution at 2000 iterations

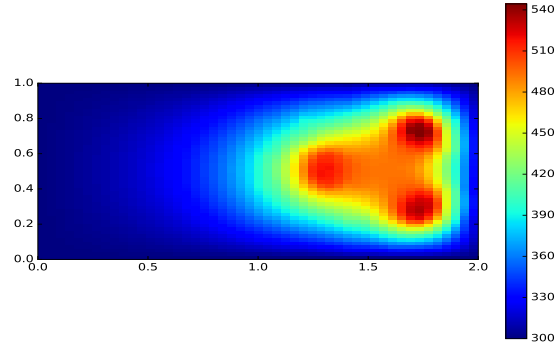


Figure 14: Final Temperature distribution at 2410 iterations

2.2 Part b: Operator Construction

The figures below show the spy plots for the operators $An2cv$ and $Acv2n_int$ respectively. By looking at the spy plot, one can clearly distinguish between the parts of the matrix responsible for handling the triangle elements (spread of matrix elements) and those handling the square elements (characterised by diagonal arrangement of elements)

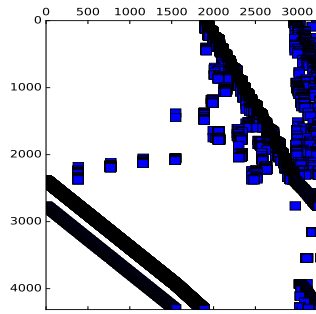


Figure 15: Spy plot of $An2cv$

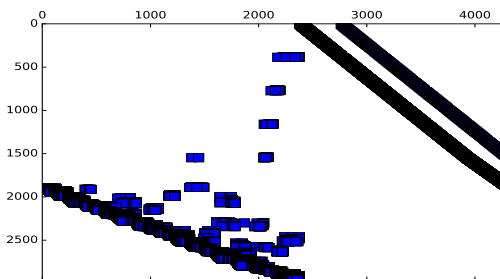


Figure 16: Spy plot of $Acv2n_int$

2.3 Extra Problem

In order to calculate the speed-up due to operator generation, the poor man's heat transfer solution was calculated for 500 iterations (should not matter since time per iteration should remain the same even if

a higher number of total iterations is considered). The following table shows the time required for each mesh through operator generation and loop implementations in parts b and a respectively.

Mesh	Time (s) (for looping)	Time (s) (operator construction)
Mesh A	5.122	0.1626
Mesh B	21.34	0.6645
Mesh C	123.8	5.387
Mesh D	271.6	16.08

Table 1: Table showing speed-up for 4 mesh sizes using Operator construction and explicit 'for' looping

3 Problem 3

3.1 Part a

The velocity field chosen for this example was

$$\vec{V} = x^2 y \vec{i} - xy^2 \vec{j} \quad (1)$$

The following quiver plot shows the velocity distribution over Mesh A

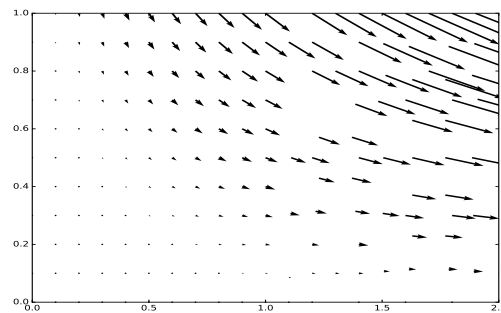


Figure 17: Quiver Plot of Velocity over Mesh A

Upon calculating the divergence using explicit looping over all the control volumes, the following flooded contours are obtained

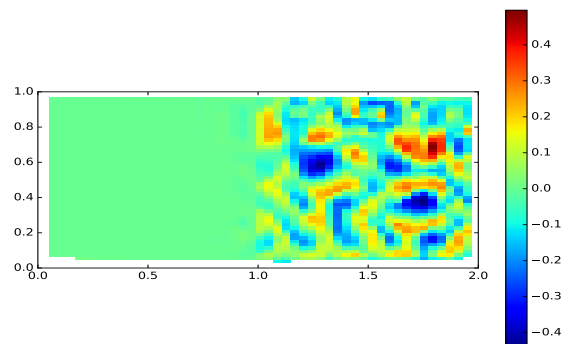


Figure 18: Flooded Contour of Divergence of velocity over Mesh A

Here, one can see that the estimation of divergence (0 in this case) improves as the mesh is refined.

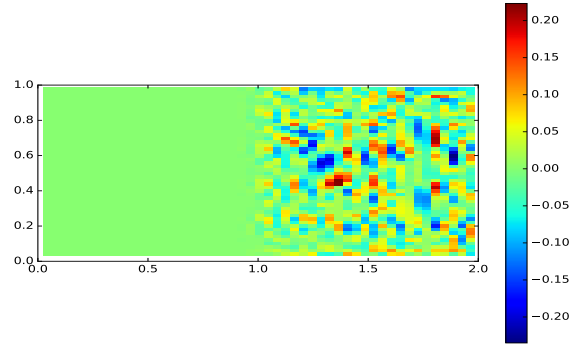


Figure 19: Flooded Contour of Divergence of velocity over Mesh B

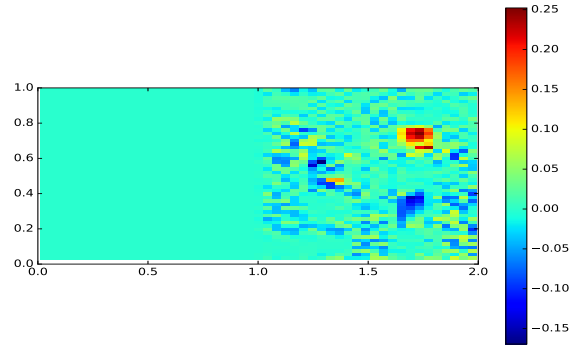


Figure 20: Flooded Contour of Divergence of velocity over Mesh C

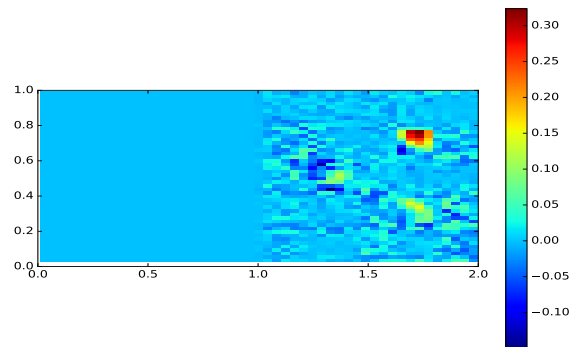


Figure 21: Flooded Contour of Divergence of velocity over Mesh D

Correspondingly, the RMS error shows first order decay when plotted against total number of control volumes.

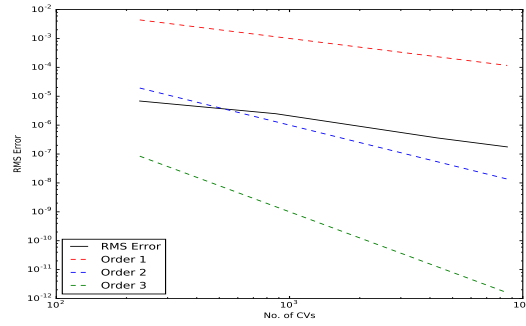


Figure 22: RMS Error decay with number of control volumes

3.2 Part b

The following figures show the spy plot for the Divergence matrices Dx_n2cv and Dy_n2cv for all 4 mesh sizes.

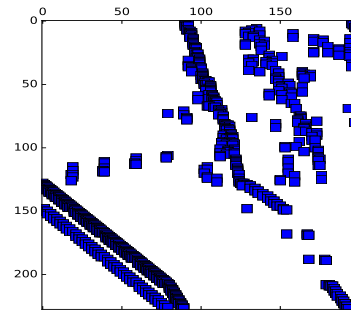


Figure 23: Spy Plot for operator Dx_n2cv for Mesh A

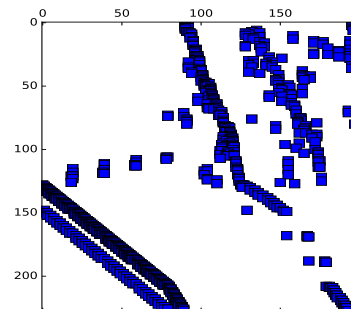


Figure 24: Spy Plot for operator Dy_n2cv for Mesh A

As verification that both methods, namely operator generation and explicit calculation over all CVs yield nearly identical numerical results, an additional flooded contour showing the absolute difference between the computed divergence values at each cell centre is also shown for Mesh C in the figure below.

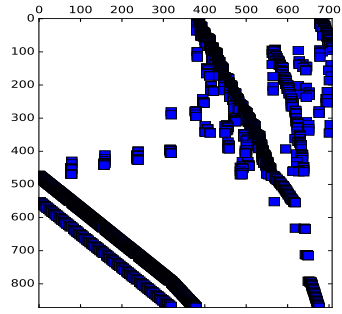


Figure 25: Spy Plot for operator Dx_n2cv for Mesh B

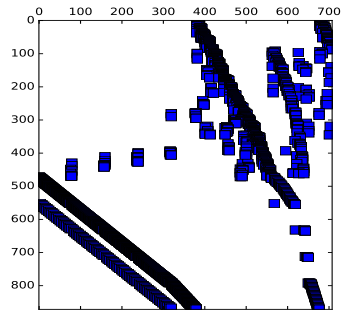


Figure 26: Spy Plot for operator Dy_n2cv for Mesh B

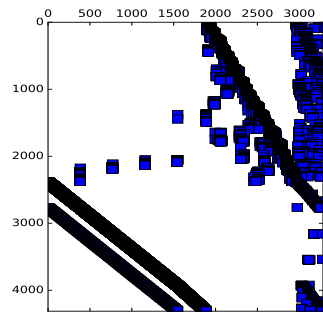


Figure 27: Spy Plot for operator Dx_n2cv for Mesh C

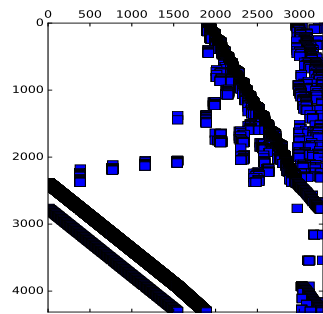


Figure 28: Spy Plot for operator Dy_n2cv for Mesh C

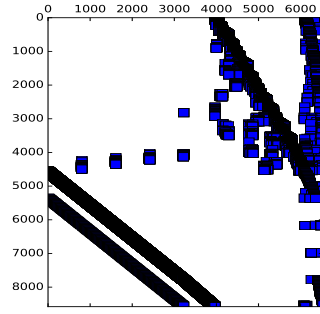


Figure 29: Spy Plot for operator Dx_n2cv for Mesh D

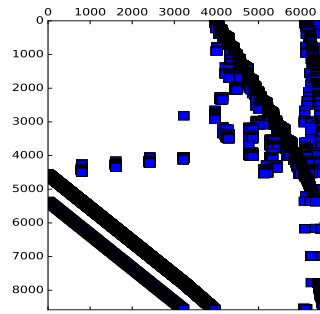


Figure 30: Spy Plot for operator Dy_n2cv for Mesh D

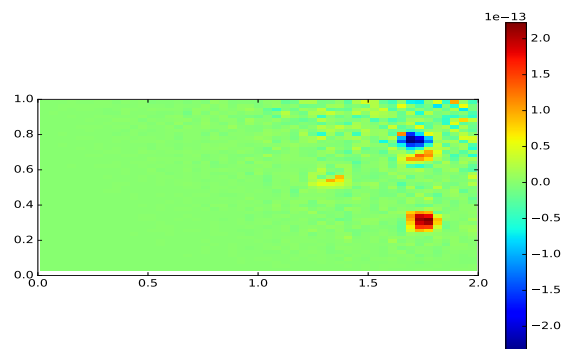


Figure 31: Flooded Contour of Divergence of velocity over Mesh D